AUTOMATED CRATER MORPHOLOGY CHARACTERIZATION ON THE MOON USING AN UNSUPERVISED NEURAL NETWORK. S. Cuevas-Quiñones[1] (cuevas26@purdue.edu), A. M. Bramson[1], and L. Rubanenko[2,3], [1]Purdue University, [2]Technion Institute of Technology, Israel. [3]Stanford University.

Introduction: Impact craters are one of the most predominant geological features on the Moon. Craters provide windows into a planet's geology, and their morphologies provide important information into the properties of the body that was impacted, and processes that have occurred since the crater formed. While previous lunar crater classification has been done by hand, it can be time consuming given the sheer number of craters that are on the Moon. We propose the use of unsupervised machine learning techniques for a more systematic approach to crater characterization. Unsupervised machine learning techniques deal with finding patterns in unlabeled data. One of their main purposes is to achieve a form of dimensionality reduction, that is, condensing data into less features while still retaining its most important aspects. Using the python deep learning packages Keras and Tensorflow, we construct an autoencoder to categorize the morphology of simple craters and explore the natural clustering that results when crater images are put through the autoencoder.

Methods: We created a trial data set composed of 46 images of craters, obtained by the Lunar Reconnaissance Orbiter Camera Wide Angle Camera (LROC WAC). To mitigate biases related to illumination, we crop images from the WAC global mosaic, which employs data obtained over multiple orbits to even out differences in solar incidence angle. Our code uses coordinates and diameters of craters manually identified on the Moon [1], reprojects the mosaic in cylindrical coordinates centered around the crater center, and crops a square region around the crater with sides equal to 1.25 crater radii. Figure 1 shows the locations of craters that were used for this initial preliminary study. Once the crater images are extracted, the images were resized to be the same number of pixels (95 × 95). A sample of these images for four different craters can be seen in Figure 2. The images are then put through an autoencoder neural network where they are first encoded, or compressed, into a set of features which is called the 'bottleneck' layer or vector. This layer is subsequently used to decode, or reconstruct, the original input. Following this step, we plot the locations of each crater within the outputted latent space of the bottleneck layer of the autoencoder. This bottleneck layer is able to identify the aspects of most variance in each image, therefore theoretically plotting images with similar features close to one another.

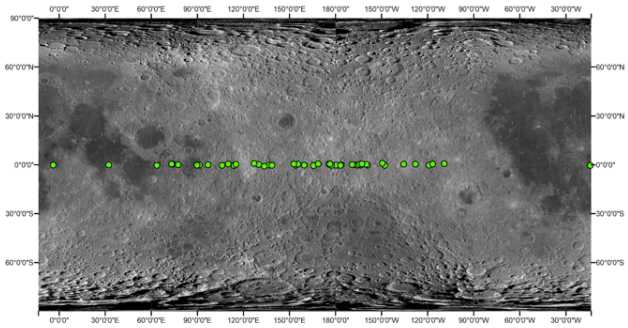

Figure 1. Locations of crater images (green dots) used for trial 1 over LROC Mosaic.

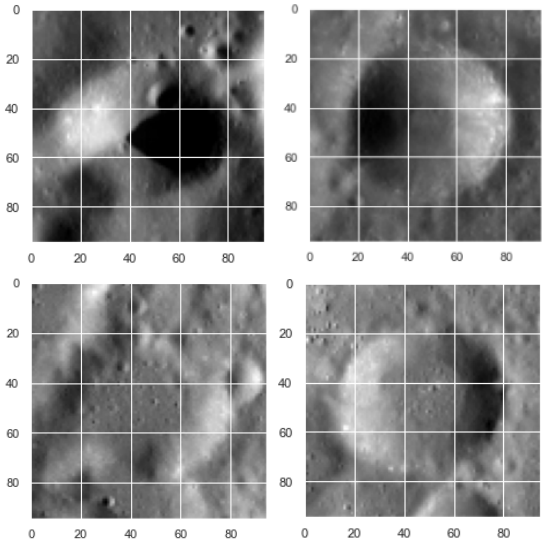

Figure 2. Examples of resized images extracted with MATLAB script to be put through the autoencoder.

For the second trial, which is currently ongoing but we plan to present the results of at the conference, we are compiling small mosaics of LROC Narrow Angle Camera (NAC) images for 100 craters. 50 of these craters are cold spot craters, which are younger, smaller, and thermophysically distinct [2], and the other 50 are non-cold spot craters of

similar size (<5 km diameter). Similarly, these will be put through the autoencoder to evaluate the viability of using an autoencoder for automated detection of morphologies that distinguish cold spot craters from older, and non-cold spot, craters.

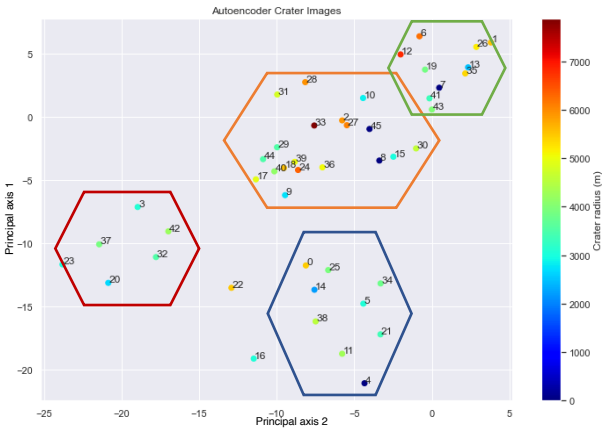

Figure 3. Decoded data plot from trial 1 (N=46). Each point corresponds to an image and numbering relates to index of each image as it was put through the autoencoder and color to crater radius. Hexagons were drawn after for clustering visualization, and we suggest four major clusters (labeled as red, blue, orange and green hexagons).

Results: The result of the first trial is shown in Figure 3. In this first trial, we have identified approximately four distinct clusters, each one having its own set of characteristic properties. Figure 4 shows a crater image example from each cluster. We find that all craters in the red cluster are well-defined and mostly circular. Outlying craters (indexed 22 and 16) that fell in the parameter space in between our four clusters also have similar features to this red cluster. The blue cluster contains degraded craters with smaller craters imposed on their interiors. Interestingly, craters of index 11, 21, and 4 (Figure 5) all had breached crater rims, and we find that most craters within the blue cluster lie on the edges of lunar maria. We find that craters within the yellow cluster are degraded and irregularly shaped; in many of these crater images, other noticeable morphological features such as a double rims, open rims, and imposed craters are also present, therefore also demonstrating their detectability by the autoencoder. The green cluster was most similar to the red cluster, with the main difference being the craters are more irregularly shaped. In respect to crater radius, we find no correlation.

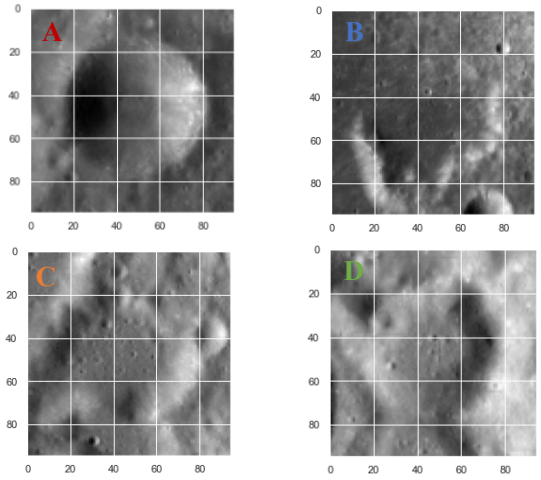

Figure 4. Craters of index 37 (A), 0 (B), 36 (C), 41 (D) each correspond to a different cluster indicated by the color of the label.

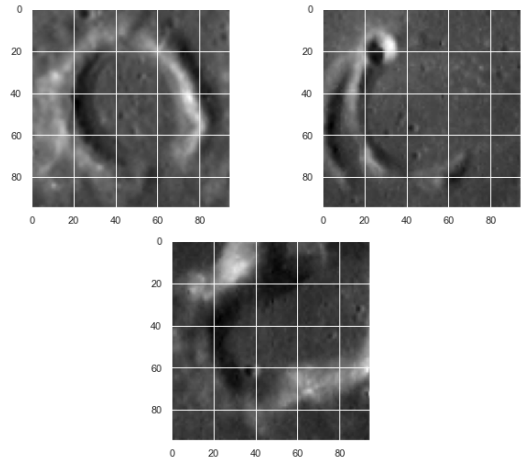

Figure 5. Degraded, breached rim craters (index 11, 21, and 4 respectively) from the blue cluster.

Future Work: Trial two is underway, where we will be able to compare cold spot crater images with non-cold spot images from LROC-NAC. The autoencoder technique is much more time-efficient than manually identifying classes and morphological properties of craters. Future modifications of the autoencoder will address characterizing other physical variables while adjusting hyperparameters and will also incorporate other data sets to identify variance in properties, such as rock abundance, radar properties, and thermal differences.

References:

[1] Robbins S. (2018) *JGR Planets, 124,871–892.*
[2] Williams J.-P. et al. (2018) *JGR Planets, 123, 2380–2392.*